Dr P A Robertson

4B13 2016

1(a)

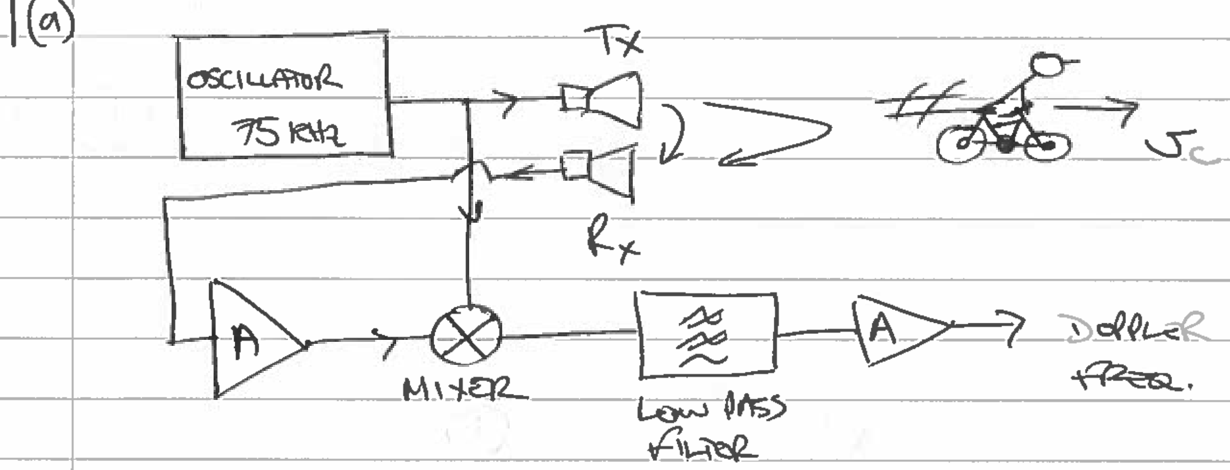

@ 75 kHz, $\lambda = \frac{340}{75{,}000} = 4{\cdot}53 \times 10^{-3}$ m

Every $\lambda/2$ distance by cyclist gives 1 Doppler cycle

$$[25\%] \quad \therefore f_{Dop} = \frac{v_c}{\lambda/2} = \frac{2v_c}{4{\cdot}53 \times 10^{-3}} = \underbrace{441 \text{ Hz} / \text{ms}^{-1}}_{\left(= 2f \frac{v_c}{v_s}\right)}$$

(b) Assume cyclist back-scatters u/sonic isotropically into hemi-sphere

U/sonic Tx power coupled into air $= \frac{\overset{24}{V^2}}{\underset{150}{R}} \cdot \overset{0.15}{\eta} \cdot \frac{\overbrace{4 Z_T Z_{AIR}}^{0.603}}{(Z_T + Z_{AIR})^2} = 0{\cdot}347$ W

$(Z_{AIR} = 340 \times 1{\cdot}2 = 408$ Ryls$)$

Range	Atten. (both ways)		Beam area
10m :	$0{\cdot}25 \times 2 \times 10 = 5$ dB	$= \times 0{\cdot}316$,	$9{\cdot}78$ m²
20m :	$0{\cdot}25 \times 2 \times 20 = 10$ dB	$= \times 0{\cdot}1$,	$39{\cdot}1$ m²

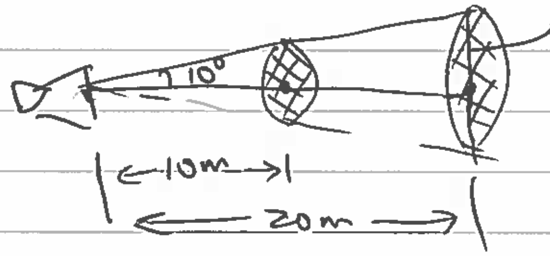

r = tan 10° × range

$A = \pi r^2$

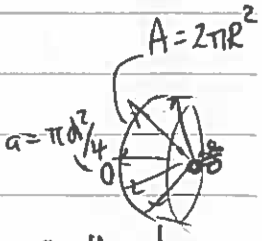

$\therefore \frac{a}{A} = \frac{\pi d^2}{4 \times 2\pi R^2}$

Assume $Z_{cyclist}$ is very different to Z_{air} $\therefore$ total reflection

Scatter

1(b) contd.

∴ Power scattered back to R_x ⇒

@ 10m : $0.347 \times 0.316 \times 0.5 / 9.78 \times 0.05^2 / 8 \times 10^2 = 17.5\,\text{nW}$

@ 20m : $0.347 \times 0.1 \times 0.5 / 39.1 \times 0.05^2 / 8 \times 20^2 = 0.35\,\text{nW}$

Coupled back to R_x and converted to electrical signal

1kΩ loaded o/cct

10m : $17.5 \times 10^{-9} \times 0.603 \times 0.5 = V_s^2 / 1000$ ∴ $V_s = 1.25\,\text{mV} \Rightarrow 2.5\,\text{mV}$

20m : $0.35 \times 10^{-9} \times 0.603 \times 0.5 = V_s^2 / 1000$ ∴ $V_s = 0.18\,\text{mV} \Rightarrow 0.36\,\text{mV}$

[35%] signal voltage amplitude

(c) $R = R_0 e^{-\beta'/T}$ @ 273K (0°C) $1000 = R_0 e^{\frac{3800}{273}}$

∴ $R_0 = 9.01 \times 10^{-4}\,\Omega$

T (°C)	V thermistor
0	2.00
10	1.22
20	0.773 ⟸ avg.
30	0.504

Take slope mid-range @ 20°C (or can use 10°C; will be larger non-linearity) ↓

$$\frac{dR}{dT} = \frac{-\beta' R_0}{T^2} e^{\beta'/T}$$

$$= \frac{-3800 \times 9.01 \times 10^{-4}}{293^2} e^{\frac{3800}{293}} = -17.1\,\Omega/°\text{C} \text{ or } -29.0\,\Omega/°\text{C}$$

× current @ 0.002 A ⇒ $-34.2\,\text{mV}/°\text{C}$ or $-58.0\,\text{mV}/°\text{C}$

∴ over 20°C range (10 - 30) ⇒ $\overset{-1.16\,\text{V}}{-0.684\,\text{V}}$ linear signal change

i.e. $1.22 - 0.684 = 0.536\,\text{V}$

[25%] ∴ non-linearity $= \left| \frac{\overset{0.504 - 0.060}{0.504 - 0.536}}{\underset{1.16}{0.684}} \right| = 0.047$ or 4.7%

0.38 or 38%

(d) $$f_{dop.} = \frac{v_c}{3 \times 10^8} \times 2 \times 24 \times 10^9 = 160\,\text{Hz}/\text{ms}^{-1}$$

[15%] will be more accurate as speed of light changes much less than speed of sound (proportionately)!

2(a) Surface micro-maching involves construction of devices onto a silicon (usually), quartz or glass substrate by deposition and patterning of consecutive layers. A sacrificial layer of polymer (photoresist), metal or silicon oxynitride can be used to provide temporary support in device fabrication and then be removed later by reactive ion etching (RIE) or wet chemical processes. Structural layers of polysilicon are produced by chemical vapour deposition (low pressure gas reactions) at elevated temperatures 200°C+ and/or plasma assist to dissociate silane SiH_4 into $Si + H_2$.

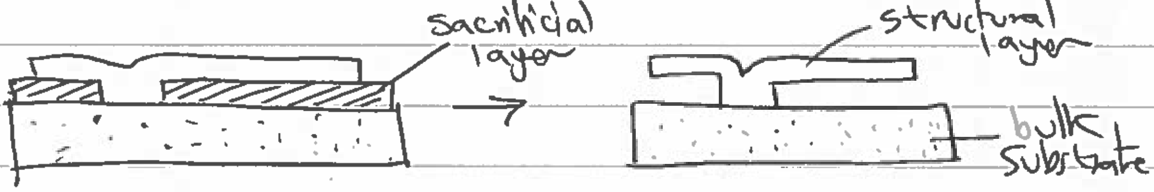

for dry etching, a plasma comprising $CF_4 + O_2$ can etch Si and SiO_xN_y films using reactive ions to create directional or more isotropic etch conditions (for steep sides on features). when creating large structures, such as the proof mass for an accelerometer, holes are patterned in the layer to allow erosion underneath to reach the sacrificial layer.

A key technique in all these steps is the use of photo-lithography: spin on a polymer layer and selectively expose to UV light through a pattern mask. The UV exposure makes the photoresist polymer more or less soluble in the developer solution. Hence positive or negative patterns of the mask can be replicated. The photoresist is then used as an etch barrier for patterning the functional layers.

Monolithic integration of MEMS with CMOS electronics reduces the effects of parasitic capacitance by having short connections between the device and interface electronics. This improves signal-to-noise ratio and allows detection of v. small displacements and currents.

[30%]

2(b) In open-loop mode an accelerometer proof mass deflects on a spring suspension, where the deflection is monitored by a differential capacitance arrangement of electrodes. The imbalance causes an output voltage – but it is only linear for small deflections. In closed loop mode, an additional set of capacitance plates maintains the proof mass in a fixed location by applying feedback forces, from voltages applied to the plates. The electronic feedback is more complex to implement, but improves linearity and signal processing can increase the apparent stiffness of the spring suspension – so raising the resonant frequency of the spring-mass system, resulting in higher bandwidth.

[15%]

2(c)(i) $$f_{res.} = \frac{1}{2\pi}\sqrt{\frac{\overset{10\ \mathrm{N\,m^{-1}}}{s}}{\underset{2\times10^{-9}\ \mathrm{kg}}{m}}} = \underline{11.25\ \mathrm{kHz}}$$

$$F = ma = 2\times10^{-9}\,.\,20 = s.x = 10x \Rightarrow x = \underline{4\ \mathrm{nm}}$$

[20%]

(ii) $$\text{total capacitance, } C_t = \frac{A\overset{8.854\times10^{-12}\ \mathrm{F/m}}{\epsilon_0}}{\underset{10^{-6}\,\mathrm{m}}{d}} = \frac{100\,.\,600\times10^{-6}\,.\,7\times10^{-6}\,\epsilon_0}{10^{-6}}$$

$$\therefore C_t = 3.72\ \mathrm{pF} \quad \text{so} \quad C_{sense} = 1.86\ \mathrm{pF} = C_{force}$$

$$F = \frac{dE}{dx} \quad \text{where } E = \tfrac{1}{2}CV^2,\ C = \frac{A\epsilon_0}{x}$$

$$\therefore \frac{dC}{dx} = \frac{-A\epsilon_0}{x^2} = \frac{C}{x} \Rightarrow F = \frac{1}{2}\frac{C}{x}V^2$$

to balance accel. $F = ma = 2\times10^{-9}\,.\,20 = 40\ \mathrm{nN}$

[20%] so with $C = 1.86\ \mathrm{pF},\ x = 1\ \mu\mathrm{m} \Rightarrow \underline{V = 0.207\ \mathrm{V}}$

(iii) 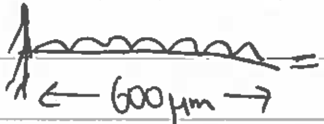

$$= \delta = WL^3/8EI \qquad W = \frac{40\times10^{-9}}{50} = 8\times10^{-10}\ \mathrm{N}$$

$E_{Si} = 140\times10^{9}\ \mathrm{Pa}$

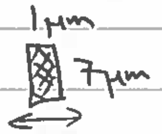

$I = \frac{1}{12}bd^3 = 5.83\times10^{-25}\ \mathrm{m^4}$

[15%]

$$\therefore \underline{\delta = 0.26\ \mu\mathrm{m}}$$

3(a)

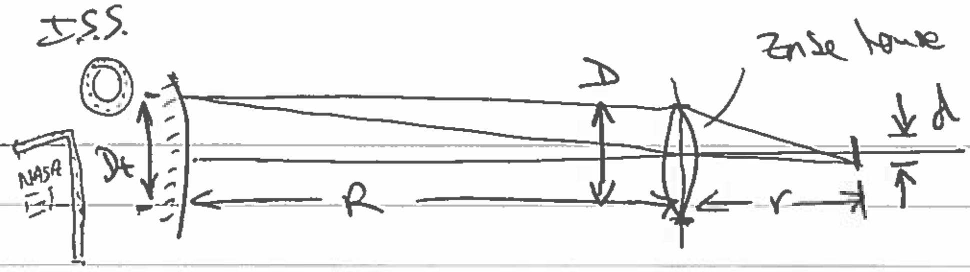

$$W = \epsilon \sigma_{SB} T^4 \qquad D = 0.05\ \mathrm{m}$$

$$\delta W = W \frac{\pi}{16} \frac{d^2 D^2}{r^2} \qquad r = 0.1\ \mathrm{m}$$

$$d = 0.005\ \mathrm{m}$$

$T = 173$ or 373 K $\qquad R = 10\ \mathrm{m}$

$$\therefore\ \delta W = 0.5 \,.\, 5.67\times10^{-8} \,.\, T^4 \,.\, \frac{\pi}{16} \,.\, \frac{0.005^2 \,.\, 0.05^2}{0.1^2}$$

round pixel $= 3.48\times10^{-14}\, T^4$ $\Rightarrow$ 31 μW to 674 μW

[25%] square pixel $4.43\times10^{-14}\, T^4$ ie: change 643 μW

(b) By similar triangles: $\frac{D_t}{R} = \frac{d}{r}$

$\frac{\times 4}{\pi} \Rightarrow$ 818 μW

$$\therefore\ D_t = 10 \,.\, \frac{0.005}{0.1} = 0.5\ \mathrm{m}$$

This is divided into 100 pixels = 5 mm/pixel on surface

[10%] of space station ∴ can see 5 mm min. feature size

(c) (i)

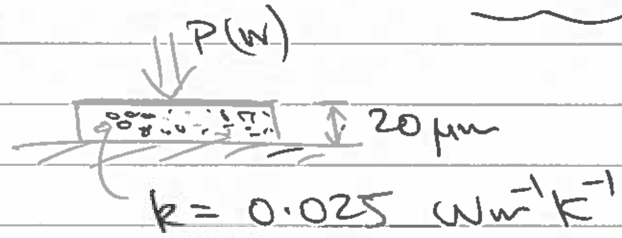

sensor temp. rise, ΔT

$$P = \frac{k A \Delta T}{d} \quad \therefore\ \frac{\Delta T}{P} = \frac{d}{kA} = \frac{20\times10^{-6}}{0.025 \,.\, 25\times10^{-6}} = 32\ ^\circ\mathrm{C/W}$$

from (a)

$$\delta W = 3.48\times10^{-14}\, T^4 \Rightarrow \begin{matrix} 193\ \mu\mathrm{W}\ @\ 0^\circ\mathrm{C} \\ 223\ \mu\mathrm{W}\ @\ 10^\circ\mathrm{C} \end{matrix} \Big\rangle\ \Delta P = 30\ \mu\mathrm{W}$$

$$\therefore\ V_{sens} = 30\times10^{-6} \,.\, 32 \,.\, 50\times10^{-6} = 48\ \mathrm{nV}$$ for 10°C change.

[20%]

or $\frac{\times 4}{\pi} = 61\ \mathrm{nV}$

3(c)(ii) we need the thermal time constant for the sensor array:

temp. difference across polymer layer

$$\text{Heat flux, } F = \frac{kA\,\Delta T}{d} = m c_p \frac{dT}{dt} \quad \text{where } \Delta T = T_\infty - T$$

$$\text{So, } \frac{kA(T_\infty - T)}{m c_p d} = \frac{dT}{dt} \quad \text{with } \tau = \frac{m c_p d}{kA}$$

$$\text{and } T' = \frac{T - T_\infty}{\tau}$$

$$-T' = \tau \frac{dT'}{dt} \quad \text{soln. } \ln T' = -\frac{t}{\tau} + C$$

Boundary conds $T = T_0$ @ $t=0$

$T = T_\infty$ @ $t = \infty$

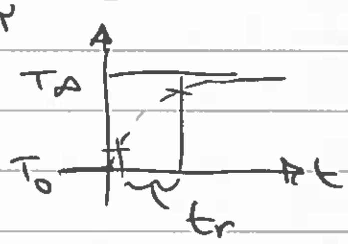

$$\therefore T = (T_0 - T_\infty)\, e^{-t/\tau} + T_\infty$$

So, the rise-time $t_r = 2.2\tau$ and $f_{-3dB} \approx \frac{1}{2\pi\tau}$

for NiCr

$$\text{Hence, with } \tau = \frac{m c_p d}{kA} = \frac{10^{-6}\ 450\ 20\times10^{-6}}{0.025\,(5\times10^{-3})^2} = 14\,\text{ms}$$

[20%] So, $f_{-3db} \simeq 11$ Hz max. response rate

($t_r = 32$ms)

(d)

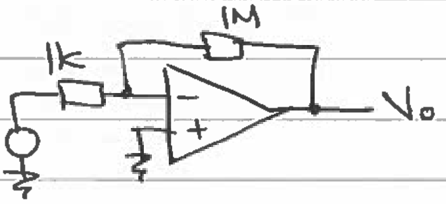

$B = 11$ Hz, $T = 273$ K

$k = 1.38\times10^{-23}$ J/K

Vnoise input	Gain	Vn out (μVrms)
$\sqrt{4kTRB}$, 1kΩ	×1000	12.9
—"—, 1MΩ	×1	0.41
$10^{-9}\sqrt{B}$, v_n	×1000	3.32
$0.3\times10^{-12}\times R\sqrt{B}$, i_n	×1000	0.99

$$\sqrt{\Sigma v_n^2} = 13.4\,\mu V_{rms}$$

(total noise)

From part (c)(i) signal $\simeq$ 6.1 nV/°C ×1000 gain = 6.1 μV/°C

[25%] $\therefore$ min. detectable $\Delta T \approx 13.4/6.1 \simeq 2$°C

4(a)

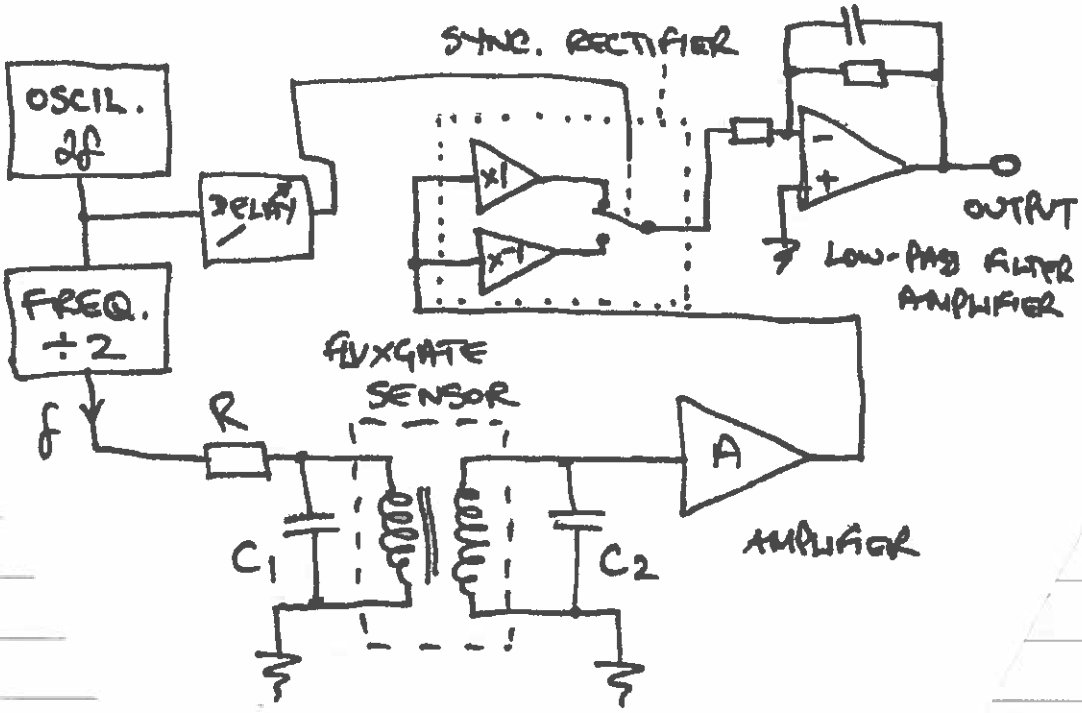

The flux-gate magnetometer utilises a saturable magnetic core periodically excited with a drive waveform via a coil coupled to the core. Another winding, or the same coil, monitors the flux in the core via an induced voltage waveform. If an external field also couples to the core, then an offset is introduced into the B-H characteristic – resulting in even harmonics being induced in the sensing coil voltage. The magnitude of these even (usually 2nd) harmonics is proportional to the external field. [20%]

(b) $f_g = 10 \times 10^3$ Hz

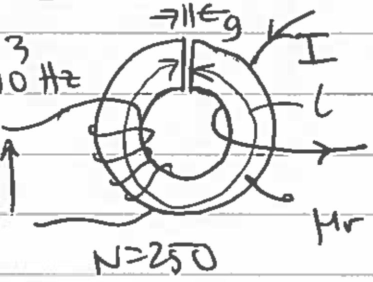

$g = 0{\cdot}25 \times 10^{-3}$ m
$l = 25\pi \times 10^{-3}$ m
$A = 80 \times 10^{-6}$ m^2
$\mu_r = 7500$

$$B = B_{air} = B_{core} = \mu_0 H_{air} = \mu_0 \mu_r H_{core} \qquad I = l H_{core} + g H_{air}$$

$$\therefore \quad I = H_{air}\left(l/\mu_r + g\right) \Rightarrow B = \frac{\mu_0 I}{\left(l/\mu_r + g\right)}, \quad \phi = BA$$

$$V_s = N\frac{d\phi}{dt} = \frac{N\mu_0 A I}{\left(l/\mu_r + g\right)} \cdot \frac{2\pi f_g}{2} \cdot \frac{2}{\pi}$$

↑ set by gating drive $\simeq 2\pi f \phi$

↑ ÷2 as only 1 core

↑ sync. rect. average of ½ sine

$\mu_{eff} = 3846 = \frac{1}{2.60\times10^{-4}}$

4(b) contd. $v_s = \frac{250 \,.\, 4\pi\times10^{-7} \,.\, 80\times10^{-6} \,.\, \cancel{\pi} \,.\, 10^4}{\underbrace{\left(\frac{\pi\times25\times10^{-3}}{7500} + 0.25\times10^{-3}\right)}_{2.60\times10^{-4}}} \,.\, \frac{2}{\cancel{\pi}} \,.\, I$

$\therefore \frac{V_s}{I} = 1.93 \text{ V/A}$

[25%]

(c) $v_i = N\frac{d\phi}{dt} = 250 \,.\, \frac{d}{dt}\left(\mu_0 I / \left(\frac{l}{\mu_r} + g\right)\right) . 80\times10^{-6}$

$\therefore v_i = \frac{0.02\,\mu_0}{2.60\times10^{-4}} \cdot \frac{dI}{dt} = 9.65\times10^{-5}\,\frac{dI}{dt}$

$= 6.06\times10^{-4}\, f_I\, I$

[15%]

(d) @ 20 A → $B = \frac{\mu_0 . 20}{(2.60\times10^{-4})} = 0.0967$ T in gap

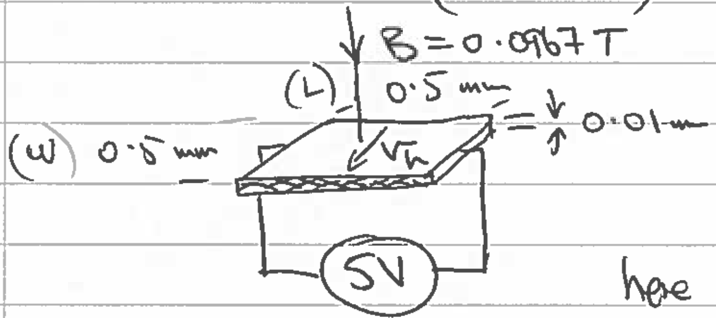

$v_h = 0.2$ V/T

Hall sensor carrier force balance: $\frac{v_h}{w}\cancel{q} = \frac{BV\mu\cancel{q}}{L}$

here $w = L$ $\therefore v_h = BV\mu$

[20%] $\therefore v_h = 0.0967 \,.\, 0.16 \,.\, 5 = 77.4$ mV

(e) In order to remove the freq. dependency of the induction coil signal, there is a requirement for a 1/f response ie: an integrator in that signal path

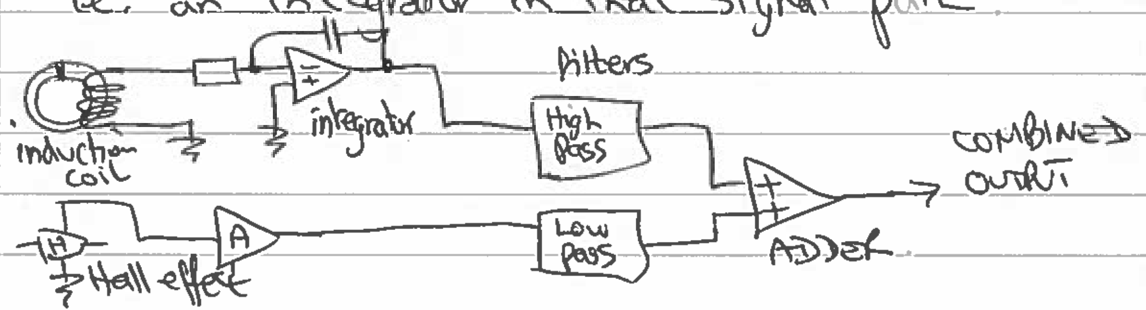

From notes, for Hall sensor simple diffusion analysis $\tau = \frac{w^2}{8D}$ where $D = \mu kT/q$ and $f_{-3dB} = \frac{1}{2\pi\tau} = 20.6$ kHz, so induction coil signal should cut in above ≃ 20 kHz

[20%]

Q1 Ultrasonic Doppler sensing and thermistors

A popular question which was well answered by most. The Doppler system schematic was fairly straightforward and most candidates made a good attempt at calculating the received signal levels, although a few omitted to apply the attenuation in both directions. The non-linearity of the thermistor signal was not well derived in many cases and, in the last part, few realised that the speed of light varies less proportionally than the speed of sound does over typical environmental conditions.

Q2 MEMS fabrication, device resonance & noise

A quite well-answered question on MEMs fabrication (surface micro-machining), with most candidates knowing the main steps, however process details were often missing. The estimate of resonant frequency was also generally well done, but few calculated the beam deflection correctly in the final part. The sensing voltage feedback was generally quite well understood.

Q3 Pyrometer system and electronics noise budget

A very popular question, which was well answered in most cases. The pyrometer analysis was generally correctly done assuming either square or round pixels; both were acceptable. The final part on circuit noise was well answered by many candidates, although the bandwidth assumptions were sometimes a little wide of the mark .

Q4 Fluxgate & Hall effect current sensors

This was the least popular question, but which attracted some high quality attempts - although some candidates failed to calculate the flux density and Hall sensor responsivity correctly. Many recalled the Hall effect sensor equations – or at least remembered the end result to use for the bandwidth estimate. The fluxgate schematic was generally well recalled as was its responsivity equation.

P. A. Robertson (Principal Assessor)